Time–course study of different innate immune mediators produced by UV-irradiated skin: comparative effects of short and daily versus a single harmful UV exposure

Eliana M. Cela,[1] Adrian Friedrich,[1] Mariela L. Paz,[1] Silvia I. Vanzulli,[2] Juliana Leoni[1] and Daniel H. González Maglio[1]

[1]*Cátedra de Inmunología (Universidad de Buenos Aires) – Instituto de Estudios de la Inmunidad Humoral (IDEHU–CONICET), Buenos Aires, and* [2]*Instituto de Estudios Oncológicos, Academia Nacional de Medicina, Buenos Aires, Argentina*

doi:10.1111/imm.12427
Received 18 September 2014; revised 18 November 2014; accepted 24 November 2014.

Correspondence: Daniel H. González Maglio, Cátedra de Inmunología – Instituto de Estudios de la Inmunidad Humoral (IDEHU), Universidad de Buenos Aires – CONICET. Junín 956, C1113AAD Buenos Aires, Argentina.
Email: danielgm@ffyb.uba.ar
Senior author: Daniel H. González Maglio

Summary

The modulatory effects of solar UV radiation on the immune system have been widely studied. As the skin is the main target of UV radiation, our purpose was to compare the impact on skin innate immunity of two contrasting ways to be exposed to sunlight. Hairless mice were UV irradiated with a single high UV dose simulating a harmful exposure, or with repetitive low UV doses simulating short occasional daily exposures. Skin samples were taken at different times after UV irradiation to evaluate skin histology, inflammatory cell recruitment, epidermal T-cell population and the mitochondrial function of epidermal cells. The transcriptional profiles of pro-inflammatory cytokines, chemokines, antimicrobial peptides and Toll-like receptors were evaluated by RT-PCR and ELISA in tissue homogenates. Finally, a lymphangiography was performed to assess modification in the lymphatic vessel system. A single high UV dose produces a deep inflammatory state characterized by the production of pro-inflammatory cytokines and chemokines that, in turn, induces the recruitment of neutrophils and macrophages into the irradiated area. On the other hand, repetitive low UV doses drive the skin to a photo-induced alert state in which there is no sign of inflammation, but the epithelium undergoes changes in thickness, the lymphatic circulation increases, and the transcription of antimicrobial peptides is induced.

Keywords: chemotaxis; inflammation; photoadaptation; skin; ultraviolet radiation

Introduction

The skin, the largest organ of the body, is organized in two primary layers, the epidermis and the dermis. The epidermis is a stratified epithelium mainly composed of keratinocytes in different stages of differentiation. The strong interactions between these cells and the variety of lipids gathered in the upper layer of the epidermis turn the skin into an effective physicochemical barrier.[1–4] Underlying the epidermis is the dermis, a connective tissue, composed of fibroblasts, elastin and collagen fibres, where various cutaneous structures and both lymphatic and blood vessels can be found.[5,6] All over the skin, there are also different resident and migrant cells, as well as constitutive or inducible molecules of the immune system. They include keratinocytes, Langerhans cells, intraepithelial T cells, dermal dendritic cells, macrophages, neutrophils, cytokines, chemokines, antimicrobial peptides and the complement system.[7,8]

The skin, as the outermost organ of the body, is constantly exposed to physical, chemical and biological stressors. In 1978, Streilein defined the skin-associated lymphoid tissue as an integrated system in which Langerhans cells, keratinocytes, resident epidermal cells, migrating lymphocytes and draining lymph nodes all work together co-ordinately to provide the skin with

Abbreviations: β-Def-14, β-defensin 14; CRAM, cathelicidin; GAPDH, glyceraldehyde-3-phosphate dehydrogenase; IL-1α, interleukin-1α; MED, minimal erythema dose; rlUVd, repetitive low ultraviolet doses; shUVd, single high ultraviolet dose; SSR, solar simulated radiation; TNF-α, tumour necrosis factor-α; UVR, ultraviolet radiation; VEGF-α, vascular endothelial growth factor-α

immunoprotection. Since then, the skin has been considered an immune organ, and keratinocytes have been regarded as the skin's immune sentinels.[9–11]

Keratinocytes can sense and respond to different microbes and microbial components through innate immune receptors that are able to recognize pathogen-associated molecular patterns, such as Toll-like receptors 2 and 4 (TLR2 and TLR4). Moreover, these cells can also sense cell damage through the recognition of danger-associated molecular patterns by TLR3. In consequence, different intracellular signal pathways are activated, leading to the production of different innate immune mediators. Among the mediators that keratinocytes can secrete, pro-inflammatory cytokines [interleukin-1α (IL-1α)/IL-1β, tumour necrosis factor-α (TNF-α), IL-6], chemokines (CCL-20, CXCL-1, CXCL-2) and antimicrobial peptides (cathelicidins and defensins) can be found. As a consequence, other different cell types are recruited towards the skin.[12,13]

Ultraviolet radiation (UVR), part of the electromagnetic spectrum emitted by the sun, can be subdivided into UVA (315–400 nm), UVB (280–315 nm) and UVC (100–280 nm). UVC is completely absorbed by the gases in the atmosphere, while only 10% of UVB and 100% of UVA reach the surface.[14] The main target of UVR is the skin and while UVA penetrates deeper into the dermis, UVB only reaches the epidermis. UVA is responsible for sunburn, skin photoaging and wrinkle formation, whereas UVB produces direct damage to the skin macromolecules, such as DNA and proteins, and indirect damage through the production of reactive oxygen species, leading to lipid peroxidation and protein modifications.[15] Photocarcinogenesis is a consequence of both direct and indirect effects of UVB. As molecular changes occur, keratinocytes are activated by UVB, so triggering and orchestrating an immune response by the production of pro-inflammatory cytokines and chemokines that promote the recruitment and activation of different immune cells, which, in turn, contribute to the inflammatory state.[12,13] Over the last decades, the interest in studying the impact of UVR exposure on the skin has increased all over the world. This concern may be based on the strong carcinogenic effects of UVR, which is considered one of the most harmful environmental carcinogens.

Although the deleterious effects of exposure to sunlight have been widely studied,[16–18] little is known about repetitive, extremely low doses of UVR, such as the exposure to everyday sunlight during regular daily activities.

Considering this lack of information, we decided to evaluate how two different and contrasting exposures to UVR impact on the skin immune system of hairless mice. We compared a single high UV dose (shUVd, two minimal erythema doses or MEDs), simulating a harmful exposure to the sun, against repetitive low UV doses (rlUVd, 0·1 MED), representing short daily exposures. First, we analysed the effects on the skin histology, epidermal T-cell, neutrophil recruitment and the mitochondrial function of epidermal cells. Then, we evaluated the transcriptional profiles and production of different pro-inflammatory cytokines, chemokines, antimicrobial peptides, TLRs and vascular endothelial growth factor-α (VEGF-α), in both the epidermis and the dermis, at different times after UVR exposure.

It was found that shUVd produced an acute and deeper inflammatory state, characterized by the production of pro-inflammatory cytokines and chemokines and the recruitment of neutrophils to the damaged area. We observed changes in the skin architecture and function that included keratinocytes that were less metabolically active and more capable of producing superoxide anions in response to the irradiation. On the other hand, after rlUVd, the skin went into a photoadaptive state, with no inflammation at all, but with changes in the skin histology and an increase in antimicrobial peptide transcription, suggesting a 'photo-induced alert state.'

Materials and methods

Mice

Male Crl:SKH1-hrBR hairless mice between 7 and 9 weeks of age (20–25 g), purchased from Charles River Laboratories (Wilmington, MA), were housed in a 12-hr/12-hr light/dark cycle and maintained with water and food *ad libitum*.

The animals were irradiated on their backs with UV light using an 8W UVM-28 mid-range (302 nm) lamp from Ultraviolet Products (UVP, Upland, CA), which emits most of its energy within the UVB range (emission spectrum range: 280–370 nm), with a peak at 302 nm, including a 20–30% amount of UVA. The lamp irradiance was measured as 1·2 mW/cm^2 using a UVX radiometer (UVP).

The mice were irradiated on their backs with a single high dose of UVR (400 mJ/cm^2, corresponding to 2 MEDs) simulating a harmful exposure, or with four repetitive low doses of UVR (20 mJ/cm^2, corresponding to 0·1 MED), over four consecutive days, simulating daily exposures. The animals were exposed to the lamp for 6 min and 4 seconds to achieve the 400 mJ/cm^2 UVR dose, and for 18 seconds to achieve the 20 mJ/cm^2 UVR dose. Non-irradiated age-matched mice used as controls were handled in the same fashion as the irradiated animals. Each group of animals was killed at different times after irradiation: 24 hr and 192 hr. For molecular biology experiments, two additional animal groups were killed 2 and 6 hr after irradiation in order to perform a kinetic analysis. The mice were killed using a CO_2 gas chamber, and then dorsal skin tissue was obtained for histological analysis, flow cytometry and RNA extraction as well as to

prepare epidermal and dermal homogenates for cytokine and chemokine quantification.

Procedures involving animals were in compliance with the research animal use guidelines established by the Consejo Nacional de Investigaciones Científicas y Técnicas (CONICET, Argentina) and approved by the Board of Ethical Review of the Instituto de Estudios de la Inmunidad Humoral.

Histology and epidermal thickness determination

The specimens for histological examination were obtained from the skin of the irradiated area using an 8-mm punch. The samples were fixed in 4% buffered neutral formalin and embedded in paraffin. Serial paraffin sections, 5-μm thick, were prepared and stained with haematoxylin & eosin. Five different samples were evaluated per mouse. Observation and photography were performed using an Olympus BX-51 microscope (Olympus, Melville, NY) with an Olympus digital camera (Q-Color 3). Epidermal thickness was measured with Image-Pro Plus 5.1 software for Windows (Media Cybernetics, Inc., Bethesda, MD).

Myeloperoxidase detection

Neutrophil infiltration of the skin was studied by immunodetection of myeloperoxidase, which can be found in high concentrations in the cytosolic granules of neutrophils. After deparaffinization by immersion in xylene and rehydration in a graded ethanol series, the paraffin sections (5 μm) were incubated for 16 hr at 4° in a 1 : 100 dilution of a monospecific antibody against myeloperoxidase (NeoMarkers, Lab Vision Corp., Freemont, CA). Subsequently, the sections were incubated for 30 min at 37° in a 1 : 100 dilution of secondary goat anti-rabbit FITC-conjugated antibodies (Bethyl, Montgomery, TX). Finally, the sections were washed three times with PBS. Observation and photography were performed using the Olympus BX-51 fluorescence microscope.

Epidermal cell isolation and flow cytometry

Skin samples were taken from each mouse using an 8-mm punch and were incubated with 25 mg/ml of dispase (Invitrogen, Carlsbad, CA) in RPMI-1640 medium for 2 hr at 37°. After incubation, the epidermis was easily separated from the dermis. Part of the epidermis was then manually homogenized with a glass-Teflon tissue grinder (Thomas Scientific, Swedesboro, NJ), and passed through a 50-μm nylon filter. Cells were counted and prepared for flow cytometric analysis.

The following anti-mouse antibodies were obtained from BD Biosciences (San Jose, CA): Alexa 647-anti-CD4, phycoerythrin-anti-CD8, FITC-anti-CD3ε, with their corresponding isotype controls. For staining of surface markers, epidermal cells were incubated with antibodies diluted in staining buffer (PBS, 10% fetal calf serum) for 30 min at 4°, washed, and then fixed in 0·2 ml of 2% formaldehyde (in PBS). Data were acquired on a PAS III PARTEC flow cytometer (PARTEC, Görlitz, Germany) and analysed using Cyflogic1.2.1 software (CyFlo Ltd., Turku, Finland).

Mitochondrial function evaluation and superoxide production

The epidermal cells were stained with probes dihexyloxacarbocyanine iodide 30 nM ($DiOC_6$, $\lambda_{excitation}$ = 484 nm; $\lambda_{emission}$ = 511 nm) (Sigma-Aldrich, St Louis, MO) to assess mitochondrial polarization, and MitoSOX Red 5 μM ($\lambda_{excitation}$ = 510 nm; $\lambda_{emission}$ = 580 nm) (Molecular Probes, Invitrogen) to evaluate mitochondrial $O_2^{\bullet -}$ production. The cells were incubated with $DiOC_6$ 30 nM and MitoSOX Red 5 μM in PBS for 30 min at 37°. Data were acquired on the PAS III PARTEC flow cytometer and analysed using Cyflogic software.

Intravital lymphangiography

Twenty-four hours or 8 days after the single or the last irradiation, 1 μl of a 1% solution of Evans blue dye in 0·9% NaCl was injected intradermally at the inner surface of the rim of the ear to visualize the lymphatic vessels. The ears of the mice were photographed 1 and 3 min after the dye injection.

RNA extraction

For epidermal RNA extraction, two 8-mm punch biopsies from dorsal skin were used; for dermal RNA extraction, one punch biopsy was processed. The skin biopsies were treated with dispase as mentioned above. The total RNA was extracted from the isolated tissues by adding Trizol reagent (Invitrogen), with subsequent homogenization using a tissue tearor (PRO Scientific, Oxford, CT). The homogenized tissues were extracted with chloroform, followed by isopropanol precipitation on ice. The RNA pellets were washed with ethanol 75% and then resuspended in diethylpyrocarbonate-treated water. The total RNA was quantified by measuring the optical density at 260 nm, controlled for integrity on an agarose gel, and stored at −70°.

Conventional RT-PCR

The first-strand cDNA was synthesized from 2 μg of the total RNA using SuperScript III Reverse Transcriptase (Invitrogen) in a total reaction volume of 20 μl, in accordance with the manufacturer's instructions. After

reverse transcription, conventional PCR was performed using specific primers for IL-6, TNF-α, CXCL-1 (KC-1), CXCL-2 (MIP-2α), CXCL-12 (SDF-1), CCL-2 (MCP-1), VEGF-α, TLR2, TLR3, TLR4, β-defensin-14 (β-Def-14), cathelicidin-related antimicrobial peptides (CRAMP) and glyceraldehyde-3-phosphate dehydrogenase (GAPDH). The primer sequences are shown in Table 1. The PCR products were resolved by electrophoresis on a 2·5% agarose gel or a 12% polyacrylamide gel, stained with SYBR Safe probe (Invitrogen), visualized using a blue light LED transilluminator (Maestrogen, Las Vegas, NV), and photographed with an Olympus digital camera (Q-Color 3). The images obtained were analysed with IMAGE J software. The results are expressed as the ratio between the individual band quantification value and the GAPDH value.

Tissue homogenate preparation

The complete dorsal skin was immersed for 30 seconds in water at 60°. The epidermis was then scraped from the dermis using a blade. The epidermis and the dermis were homogenized using a tissue tearor (Thomas Scientific) in 1 ml (epidermis) and 3 ml (dermis) of the extraction buffer: $(NH_4)_2CO_3$ 50 mM pH 8 – Triton X-100 0.02%. After centrifugation for 10 min at 10 000 ***g***, the supernatants were lyophilized and stored at −70° until use. For cytokine and chemokine quantification, the samples were reconstituted in 200 µl of PBS. The total protein concentration in the reconstituted samples was measured with a BCA Protein Assay Reagent Kit (Pierce Biotechnology, Rockford, IL).

Table 1. Primers used to amplify mRNAs

cDNA targets	Oligonucleotides	Product size (pb)
IL-6	FW: GTGGAAATGAGAAAAGAGTTGTGC	469
	RV: ATGCTTAGGCATAACGCACTAGGT	
TNF-α	FW: GCAGGTCTACTTTGGAGTCATTGC	300
	RV: CATTCGAGGCTCCAGTGAATTCGG	
VEGF-α	FW: TATTCAGCGGACTCACCAGC	561
	RV: GAGCCCAGAAGTTGGACGAA	
TLR-2	FW: TCTGGGCAGTCTTGAACATTT	321
	RV: AGAGTCAGGTGATGGATGTCG	
TLR-3	FW: CATGATGTCGGCAACGGTTC	611
	RV: ACCCTCCTGAGCATCAGTCT	
TLR-4	FW: GCAATGTCTCTGGCAGGTGTA	406
	RV: CAAGGGATAAGAACGCTGAGA	
CXCL-1	FW: TGGCTGGGATTCACCTCAAG	179
	RV: CCGTTACTTGGGGACACCTT	
CXCL-2	FW: TCCAGAGCTTGAGTGTGACG	251
	RV: TCAGGTACGATCCAGGCTTC	
CXCL-12	FW: GCCCTTCAGATTGTTGCACGGC	338
	RV: AAAGCTCCATTGTGCACGGGCG	
CCL-2	FW: CAGGTCCCTGTCATGCTTCT	91
	RV: GTGGGGCGTTAACTGCATCT	
B-Defensin-14	FW: TCTTGTTCTTGGTGCCTGCT	87
	RV: CACACCGGCCACCTCTTATT	
Cathelicidin	FW: ATCAGCTGTAACGAGCCTGG	169
	RV: AGGCCTACTACTCTGGCTGA	
GAPDH	FW: AACTTTGGCATTGTGGAAGGGCTC	473
	RV: ACCCTGTTGCTGTAGCCGTATTCA	

FW and RV indicate forward and reverse primers.

Cytokine and chemokine quantification in the epidermis and the dermis

Murine TNF-α, IL-6, CXCL-1 (KC-1) and CCL-2 (MCP-1) from epidermal and dermal extracts were quantified using non-competitive ELISAs (BD Biosciences), according to the manufacturer's instructions. The values are expressed as pg/mg of protein.

Statistical analysis

All the values are presented as the mean ± SD. The statistical significance was evaluated using one-way analysis of variance (ANOVA). When the variables had a normal distribution and showed homoscedasticity, a parametric ANOVA and a Student–Newman–Keuls post-test were used. When samples did not have a normal distribution or showed heteroscedasticity, a non-parametric ANOVA and a Dunn's post-test were used. Graphical and statistical analyses were performed with GRAPHPAD PRISM 5.0 (GraphPad Software, La Jolla, CA) and GRAPHPAD INSTAT 2.0 (GraphPad Software), respectively. The values were considered different at $P < 0{\cdot}05$, $n = 5$.

Results

Both irradiation models produce histological alterations in the skin

As the skin is the main target of UVR, we analysed the impact of skin exposure to UVR on the integrity of the epithelium, assessing changes in the skin architecture by histology observation and alterations in the epidermal T-cell population. We then measured the mitochondrial membrane potential ($\Delta\psi m$), both as an important parameter of mitochondrial function and as an indicator of cellular metabolic activity, as well as the superoxide production by keratinocytes. Twenty-four hours after an shUVd, the epidermis was severely damaged, keeping only its basal stratum (Fig. 1a,b). The remaining keratinocytes turned into less metabolically active cells with a lower percentage of polarized mitochondria (Fig. 1c). According to the epithelial damage, keratinocytes decreased their mitochondrial $O_2^{\bullet -}$ production (Fig. 1d)

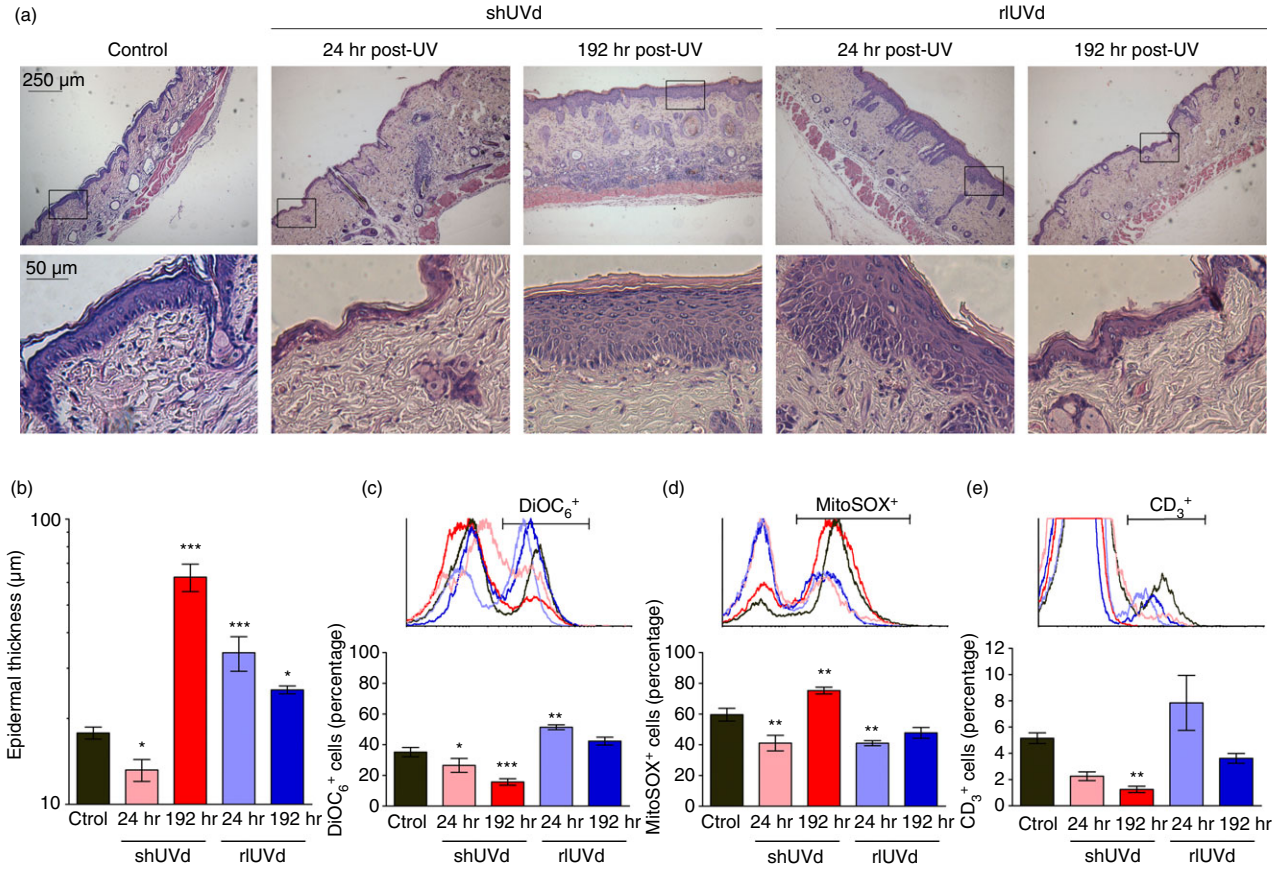

Figure 1. (a) Histological appearance of epidermal alterations produced by a single high UV dose (shUVd) and repetitive low UV doses (rlUVd) at different times after UV irradiation. (b) Epidermal thickness quantification. The values are expressed in µm. (c) Mitochondrial membrane potential detected by $DiOC_6$ staining. (d) $O_2^{\bullet -}$ production detected by MitoSOX red staining. (e) Epidermal T-cell population detected after skin exposure to an shUVd and to rlUVd, and in the non-irradiated control group. Marker indicates the region of cell population used for the analysis. The results are expressed as mean ± SD. $^*P < 0.05$, $^{**}P < 0.01$, $^{***}P < 0.001$.

and exhibited a marked but statistically non-significant reduction in the percentage of epidermal $CD3^+$ cells (Fig. 1e). Eight days (192 hr) after an shUVd, the epithelium was in a proliferative process, with an increase in the epidermal thickness (Fig. 1a,b). However, these keratinocytes were still less metabolically active, producing higher levels of $O_2^{\bullet -}$ (Fig. 1c,d). The percentage of epidermal $CD3^+$ cells was significantly decreased (Fig. 1e). Twenty-four hours after skin exposure to rlUVd, we found an epithelium in a hyper-proliferative state with a marked increase in the epidermal thickness (Fig. 1a,b). The percentage of keratinocytes with polarized mitochondria was increased, which means that cells were more metabolically active (Fig. 1c). The thickness of the epithelium showed a tendency to decrease after 8 days post-rlUVd, but was still increased compared with the control epidermis (Fig. 1a,b). No significant differences in the percentage of $CD3^+$ cells were seen at any time after rlUVd (Fig. 1e). The epidermal and dermal histological alterations after skin exposure to UVR are summarized in Table 2.

Skin exposure to an shUVD produces a marked inflammatory state

An shUVd induced the production of pro-inflammatory cytokines in a time-dependent fashion. Differences were observed in each anatomical place analysed. The dermis showed no increments in TNF-α expression at any time compared with basal production but even slight but significant decreases 2, 6 and 24 hr post-UV. Instead, IL-6 expression peaked first in the dermis 2 hr post-UV irradiation, then decreased and stayed steady but higher than control over 24 hr (Fig. 2a). Regarding the epidermis, the expression of TNF-α started as early as 2 hr after UV exposure, reaching a maximum level after 24 hr, while IL-6 appeared after 24 hr (Fig. 2b). Interestingly, using RT-PCR we could not find the RNA induction of the

Table 2. Skin histological alteration after UV radiation exposure

Irradiation	Time (hr)	Epidermis	Granuloma	Polymorphonuclear cell infiltrate	Lymphocyte infiltration
Non-irradiated	0	Thin	Epithelioid histiocytes, polymorphonuclear cells and multinucleated giant cells around hair follicles	Around hair follicles	Around hair follicles
shUVd	2	Thin	Around hair follicle	Absence	Absence
	6	Thin apoptotic cells in basal layer	Deep in dermis	Slight and diffuse	Moderate
	24	Focal erosion necrotic cells in basal layer	Around hair follicle, bigger than control, epithelioid histiocytes, and multinucleated giant cells deep in dermis	Numerous in granulomas	Interstitial infiltrate
	192	Hyperkeratosis Hyperplasia Acanthosis	Multiple granulomas around hair follicles deep in dermis	Regular number in granulomas	Great infiltrate deep in dermis
rlUVd	2	Thin	Similar to control	In granulomas	Few
	6	Slight hyperkeratosis	Similar to control	Few interstitial infiltrates	Few
	24	Acanthosis focus	Few	Around hair follicles	Few
	192	Acanthosis focus	Few	In granulomas and few interstitial infiltrates	Few

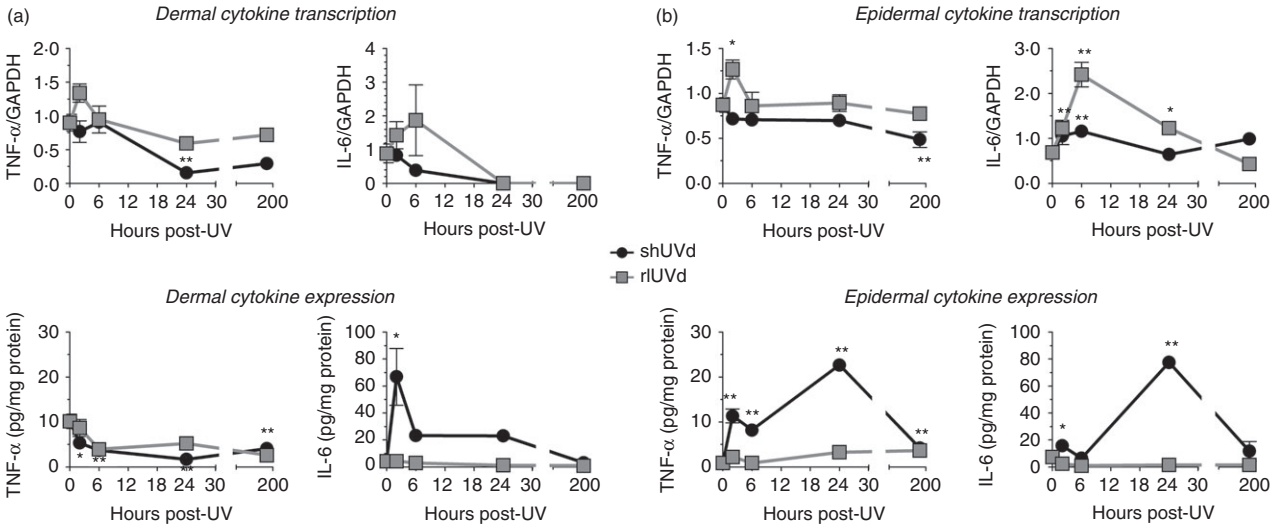

Figure 2. Tumour necrosis factor-α (TNF-α) and interleukin-6 (IL-6) mRNA transcription and protein expression in the dermis (a) and the epidermis (b) after skin exposure to a single high UV dose (shUVd) and to repetitive low UV doses (rlUVd). All measurements were performed at 2, 6, 24 and 192 hr after UV or UV mock-irradiation. The results are shown relative to GAPDH and to mg/ml of protein, and expressed as mean ± SD. $^{*}P < 0.05$, $^{**}P < 0.01$.

cytokines detected in the homogenates, probably because of a rapid transcription (within minutes) and different kinetics compared with those analysed in the present study. For certain inflammatory cytokines, a biphasic transcriptional profile has been described that may support this idea.[19] After rlUVd exposure, on the other hand, even though we saw slight increments in TNF-α and IL-6 mRNA transcription in both the dermis and the epidermis, we could not detect these cytokines in the epidermal and dermal tissue homogenates (Fig. 2a,b).

An shUVd induces infiltration of neutrophils into the dermis

As is widely known, the blood cells that arrive first at damaged tissue are neutrophils, followed by monocytes a few hours later. Consequently, we decided to evaluate the mRNA transcription and the protein expression of neutrophil chemoattractants CXCL-1 and CXCL-2 and of monocyte chemoattractant CCL-2 in the epidermis and the dermis of irradiated mice. Furthermore, the presence

of these polymorphonuclear and mononuclear cells and their distribution in the tissue were assessed.

After an shUVd, there was a quick and strong induction of CXCL-1 and CXCL-2 mRNA transcription first in the dermis and later in the epidermis, between 2 and 6 hr post-UV exposure, leading to a peak in protein expression 24 hr after UV irradiation in both tissues (Fig. 3a–d). CCL-2 mRNA transcription peaked in the dermis at 24 hr post-UV without a significant increase in epidermis (Fig. 3a,b). Consequently, the protein expression was markedly increased in the dermis 24 hr after an shUVd and slightly up-regulated in the epidermis at the same time (Fig. 3c,d). As shown in Table 2, normal SKH-1 hairless mice are characterized by the presence of granulomas around hair follicles. These granulomas are composed of macrophages and histiocytes. As a consequence of the induction of these chemoattractant molecules, an influx of inflammatory cells arrived at the dermis. Twenty-four hours after an shUVd, the size of the granulomas was increased in the irradiated area, and after 192 hr we found multiple granulomas deep in the dermis (Fig. 3e). This means that there was an influx of monocytes and macrophages, which is related to the CCL-2 expression. Furthermore, neutrophils were recruited to the affected area of the dermis 24 hr after an shUVd, and their number increased even more after 192 hr, as can be corroborated by myeloperoxidase immunofluorescence staining (Fig. 3f,g). Neutrophils appeared diffused both near the basal membrane and deeper in the dermis. No polymorphonuclear cells were observed in the epidermis of irradiated skin. In non-irradiated skin, neutrophils were absent.

On the other hand, after rlUVd we could not find CXCL-1 protein expression either in the epidermis or in the dermis, despite the induction of CXCL-1 and CXCL-2 mRNA transcription (Fig. 3a–d). These results are in accordance with the absence of polymorphonuclear cells and myeloperoxidase-positive cells in the skin histology (data not shown).

Regarding the chemoattraction of lymphocytes to the skin after UV irradiation, we decided to evaluate the transcription of CXCL-12, a lymphocyte and monocyte chemotactic factor. The dermal transcription of CXCL-12 was increased significantly in both irradiated groups (Fig. 3a), peaking at 2 hr post-UV and then decreasing. On the other hand, the transcription of this chemokine was only increased in the epidermis of rlUVd-exposed mice (Fig. 3b), with similar kinetics to the dermal transcription. CXCL-12 transcription correlated with the lymphocyte infiltration in dermis of shUVd-exposed animals, which began at 6 hr as a moderate infiltrate and evolved to a great deep infiltration at 192 hr post-UV (Table 2). However, there was little lymphocyte infiltration in the dermis of rlUVd-exposed mice, probably because of migration to the epidermis (Table 2 and Fig. 1e).

rlUVd lead to an enlargement of the cutaneous lymphatic vessels

Another important event occurring during inflammation is the increase in vascular permeability. Apart from pro-inflammatory cytokines, such as IL-6, TNF-α and IL-1β, there are other molecules involved in vascular changes, like VEGF-α. To investigate whether UVR resulted in VEGF-α induction, we evaluated VEGF-α mRNA transcription in the epidermis and the dermis after both UVR exposures. Surprisingly, we observed an induction of VEGF-α mRNA first in the epidermis, 2 hr after skin exposure to rlUVd, reaching the highest levels 24 hr post-UV irradiation (Fig. 4a). In the dermis, VEGF-α mRNA up-regulation started 24 hr post-rlUVd, with the maximum level of induction at 192 hr (Fig. 4a). There were no changes in VEGF-α mRNA in shUVd-exposed mice. To further investigate the role of UVR in the function of cutaneous lymphatic vessels, we performed an intravital lymphangiography. Thirty seconds after Evans blue injection, dilated lymphatic vessels were visualized in the rlUVd group at different points in time, indicating an enlargement of cutaneous lymphangiography (Fig. 4b). These effects were less pronounced after skin exposure to an shUVd.

rlUVd induce the transcription of antimicrobial peptides, both in the epidermis and the dermis

The mRNA transcription of TLR2 and TLR4 was checked in order to analyse possible changes in the recognition of pathogens through their pathogen-associated molecular patterns. Moreover, the transcription of TLR-3 was analysed to study changes in the recognition of cell damage signals through release of danger-associated molecular patterns. After an shUVd we found a marked down-regulation of TLR2 and TLR4 transcription in the dermis (24 and 192 hr and 6 hr, respectively) (Fig. 5a). A less pronounced effect was seen for TLR2 in the epidermis (6 and 192 hr, Fig. 5b). However, in the dermis of rlUVd-exposed mice, 24 and 192 hr post-UV there was a peak in the induction of TLR4 and TLR2 mRNA, respectively. There were no significant alterations in the transcription of TLR3 in dermis or epidermis. To examine whether these differences in TLR expression correlate with the antimicrobial responses of the tissue, we evaluated CRAMP and β-Def-14 mRNA transcription in irradiated skin. β-Def-14 mRNA transcription was highly increased 6 hr after skin exposure to rlUVd in the dermis and the epidermis (Fig. 5a,b). This antimicrobial peptide decreased after 6 hr, and stayed steady but higher than control over 192 hr post-irradiation in the dermis, returning quickly to basal levels in the epidermis (Fig. 5a, b). On the other hand, CRAMP transcription was only increased in the dermis with a maximum level of

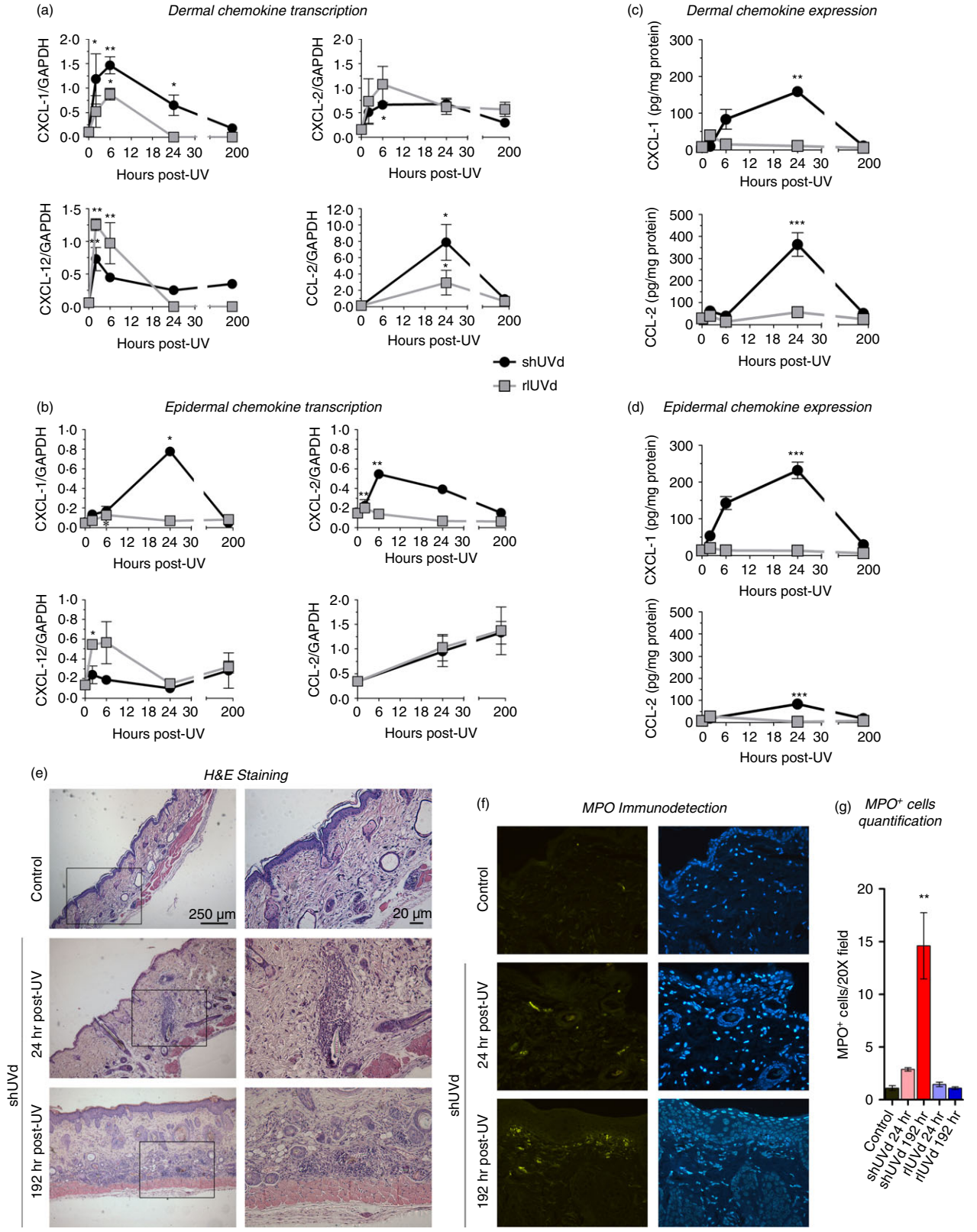

Figure 3. Chemokine (CXCL-1, CXCL-2, CXCL-12 and CCL-2) mRNA transcription and protein expression were evaluated in the dermis (a–c) and the epidermis (b–d) after 2, 6, 24 and 192 hr post-UV exposure. The results are shown relative to GAPDH and to mg/ml of protein. Dermal cellular infiltrate was evaluated by haematoxylin & eosin staining (e) and myeloperoxidase FITC staining (f) and quantification (g) of hairless mice skin sections after a single high UV dose (shUVd). DNA Höechst staining was also performed. The results are expressed as mean ± SD. * $P < 0.05$, ** $P < 0.01$, *** $P < 0.001$.

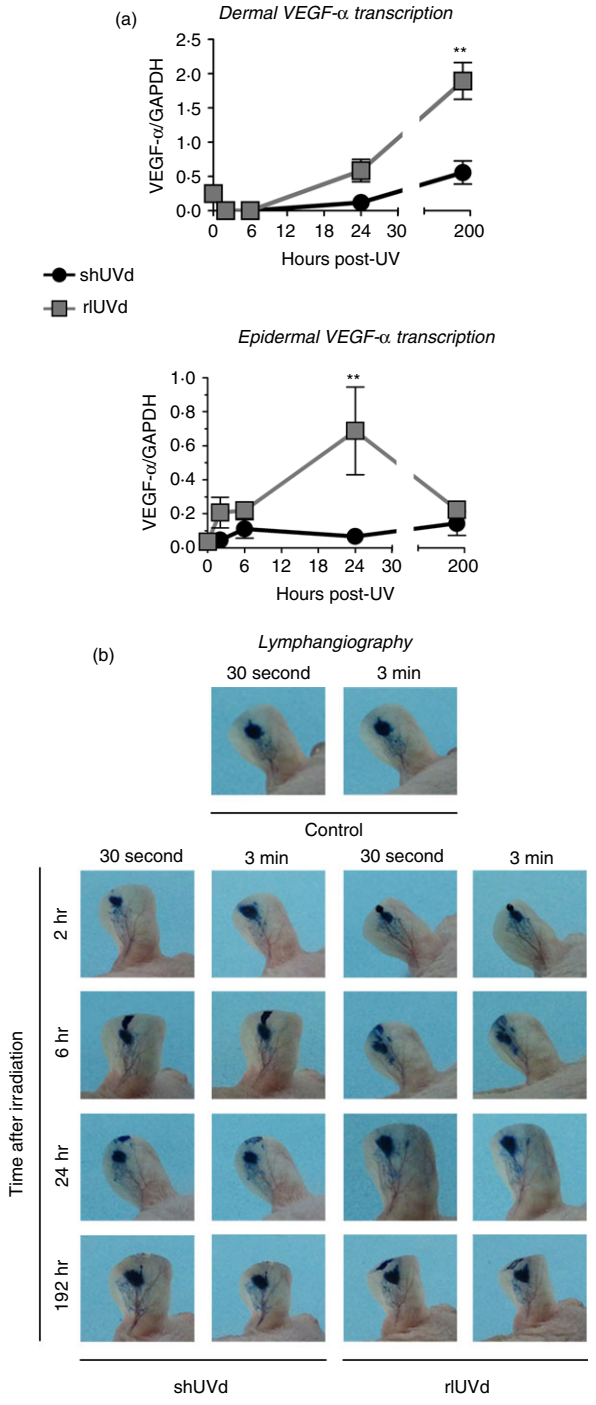

Figure 4. (a) Vascular endothelial growth factor-α (VEGF-α) mRNA transcription was evaluated in the dermis and the epidermis of mice exposed to a signle high UV dose (shUVd), to repetitive low UV doses (rlUVd) and mock-irradiated, 2, 6, 24 and 192 hr post-UV. (b) Lymphatic vessel evaluation by intravital lymphangiography. Photographs were taken 30 seconds and 3 min after Evans blue dye injection. The results are expressed as mean ± SD. $^{**}P < 0.01$.

induction 2 hr post-UV (Fig. 5a). Although skin exposure to an shUVd also induced the expression of both antimicrobial peptides in both tissues and in the same time-dependent fashion, the levels of induction reached were significantly lower than those reached by rlUVd.

Discussion

Since the studies carried out by Margaret Kripke in the 1970s, the relationship between UVR and the immune system has been considered.[20–22] Those studies showed that UV-irradiated mice were unable to reject subcutaneous implanted tumours, because of the induction of an immunosuppressive state. Moreover, irradiated mice presented impaired contact and delayed-type hypersensitivity responses, mediated by UV-induced specific regulatory T cells. From then on, plenty of research has been performed in the field of photoimmunology. Most of this research includes the study of the deleterious effects associated with UVR exposure using high doses, which simulate harmful exposures to the sun. However, we are daily and naturally exposed to the sun for short periods of time and receive low UV doses that do not burn the skin. It is worth noting that practically all the research done has evaluated different parameters of the adaptive immune system (delayed-type hypersensitivity, contact hypersensitivity, adoptive cell transfer), and has not gone into detail about the innate immune response.

In this work we aimed to compare two different and contrasting ways to be exposed to sunlight: a single harmful exposure and a daily one. We compared them by assessing the impact of UVR exposure on the skin immune system and the skin architecture, with an approach to the innate immune responses triggered by UVR.

The results of this study show, as already described, that an shUVd produces severe epidermal histological damage in a time-dependent manner, reaching a maximum level 24 hr post-exposure. At this time, the epithelium is completely disorganized, and only its basal layer remains, whose cells exhibit mitochondrial alterations with a loss of polarization and a reduction in $O_2^{\bullet -}$ production. This particular response may be related to the vast damage and also to a reduction in the oxygen uptake by the damaged mitochondria.[23] Interestingly, as epidermal cells are more damaged, as shown by a less organized epithelium and by their metabolic active reduction, they are able to produce high amounts of pro-inflammatory cytokines and chemokines, while the dermis seems to promote chemotaxis with no production of pro-inflammatory cytokines. As a consequence, there is a recruitment of neutrophils into the irradiated area. The presence of those neutrophils may contribute to the removal of damaged cells due to their phagocytic ability, probably as a repair mechanism.[24] In addition to neutrophil and monocyte infiltration, there was a lymphocyte infiltrate that may contribute to inflammation. Therefore, an shUVd produces a marked inflammatory state, as reported

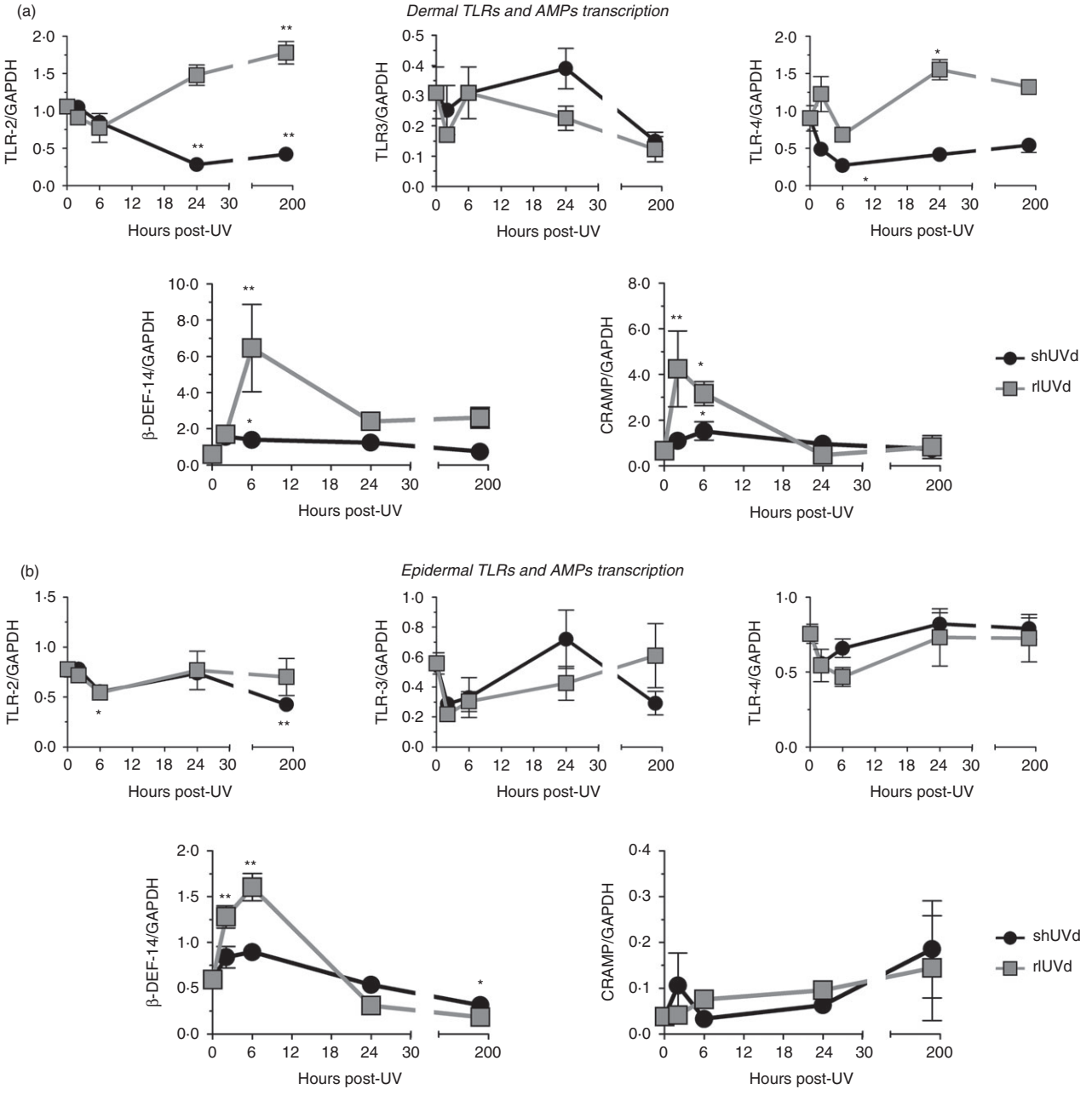

Figure 5. Transcription of Toll-like receptors (TLR2, TLR3, TLR4) and antimicrobial peptides [β-defensin 14 (β-Def-14) and cathelicidin (CRAMP)] was evaluated in the dermis (a) and the epidermis (b) after a single high UV dose (shUVd), repetitive low UV doses (rlUVd) and mock-irradiation 2, 6, 24 and 192 hr post-UV. The results are shown relative to GAPDH and are expressed as mean ± SD. $^{*}P < 0.05$, $^{**}P < 0.01$.

previously.[25–28] Nevertheless, the epidermis has the ability to recover itself, as seen 8 days post-UV, when the epithelium is in a proliferative state.

According to previous work, it is well known that UVR produces damage in DNA,[29,30] and this damage can be cumulative in basal keratinocytes. Therefore, a proliferative response of the epithelium may be a barrier to protect those basal cells against further damage. This epidermal hyperplasia is observed 8 days after shUVd, maybe as a photoprotective skin mechanism, activated after epithelial damage.

In contrast to the inflammatory response produced by an shUVd, after skin exposure to rlUVd the epidermal keratinocytes do not produce any inflammatory mediator. However, we found a rapid and intense induction of antimicrobial peptide mRNA transcription (up to eightfold) in the epidermis and the dermis. It has been reported that keratinocytes in the epidermis and fibroblasts in the

dermis are able to produce antimicrobial peptides in response to UVR *in vitro* and *in vivo*.[31] Antimicrobial peptide production by irradiated skin represents an important innate immune mechanism, necessary to defend the organism against possible bacterial infections. We would have expected to find antimicrobial peptide transcription greatly increased in the dermis of shUVd-exposed mice as well, because the epithelium is severely damaged. Nevertheless, there is an early slight induction, followed by a quick return to basal levels. Our results agree with previous studies performed by Hong *et al.*,[32] who observed beneficial effects of repetitive low-dose UVB exposure, including an increase in epidermal antimicrobial peptide expression and permeability barrier reinforcement.

Skin exposure to UVR leads to an increase in vascular permeability, leading in turn to oedema formation, through the up-regulation of angiogenic factors, such as VEGF-α.[33] Even though VEGF-α is directly associated with blood vessel angiogenesis, recent studies have shown that this factor is also involved in lymphangiogenesis during tumour development.[34] Despite the fact that the role of lymphatic vessels during inflammation is well known, the possible implications of these vessels during the skin response to UVR have not been fully studied, beyond dendritic cell migration. In our studies, we evaluated the transcriptional profile of VEGF-α and performed a lymphangiography to evaluate changes in the lymphatic vasculature. Interestingly, the epidermis produces VEGF-α mRNA as early as 2 hr post-rlUVd, and mRNA still remains up-regulated 8 days later. Although both irradiation models produce lymphatic vessel dilatation (observed after Evans blue dye injection), only after rlUVd is it possible to visualize the presence of new vessels indicating an enlargement of the lymphatic vasculature, in accordance with previous work.[35] However, we do not see any leakage of the dye.

In conclusion, our results show that there are differences between both irradiation models. An shUVd leads the skin to an inflammatory state, while rlUVd drive the skin to a 'photoadaptive state'. Photoadaptation has been defined as the 'diminished future response to equivalent doses of irradiation', but it was described just for a few effects such as erythema formation and epidermal DNA damage.[16] In response to rlUVd, we observed epidermal hyperplasia and hyperkeratosis as a sign of photoadaptation. Little research has been reported using repeated suberythemal doses, mostly performed by Norval *et al.* They irradiated mice with repetitive sub-erythemal solar simulated radiation (SSR) during 2, 10 or 30 consecutive days and challenged them on the final day with a single erythemal SSR. They observed that after repetitive exposures to sub-erythemal SSR, there was photoadaptation to the erythemal UV-induced suppression of the phagocytic activity of peritoneal macrophages,[36] but not in many other effects such as immunosuppression and alterations in Langerhans cell number and function. Such photoadaptation was evaluated after repetitive sub-erythemal UV exposures, but these were significantly higher than the doses used in this work (≈ 0·5 MED versus 0·1 MED). Moreover, the photoadaptation assessment was performed by challenging the skin with a high UV dose. Our approach to the problem was to evaluate the 'photoadapted' skin before the challenge, analysing structural and molecular alterations produced by rlUVd related to skin integrity and the innate immune mechanisms triggered. These mechanisms may protect the skin not only against a harmful UV exposure but also against other noxae such as microorganisms, which may invade the skin through the altered epithelium.

As the skin responds to rlUVd by increasing its epidermal thickness, there is no sign of inflammation. Besides, the skin increases the production of antimicrobial peptides and vascularization, so as to be prepared for potential challenges that it may have to deal with due to UV exposure.

Acknowledgements

This work was supported by the University of Buenos Aires (UBACyT 2011-2014 and CONICET PIP 2011-2013 Grants). The authors would also like to thank Ms Dolores Campos, Ms Carolina Mourelle and Ms Angélica Miranda for their technical support and advice in relation to mouse care and management and Dr Daniela Ureta for her assistance in flow cytometric analysis. Eliana Cela performed the research, designed and analysed the experiments and wrote the manuscript. Adrián Friedrich performed the research and corrected the manuscript. Silvia Vanzulli performed the histological analyses. Mariela Paz and Juliana Leoni designed the experiments and corrected the manuscript. Daniel González Maglio designed the experiments and wrote the manuscript.

Disclosures

The authors state no conflict of interest.

References

1 Simpson CL, Patel DM, Green KJ. Deconstructing the skin: cytoarchitectural determinants of epidermal morphogenesis. *Nat Rev Mol Cell Biol* 2011; **12**:565–80.
2 Proksch E, Brandner JM, Jensen JM. The skin: an indispensable barrier. *Exp Dermatol* 2008; **17**:1063–72.
3 Bouwstra JA, Honeywell-Nguyen PL, Gooris GS, Ponec M. Structure of the skin barrier and its modulation by vesicular formulations. *Prog Lipid Res* 2003; **42**:1–36.
4 Apostolos P. Epidermal surface lipids. *Dermatoendocrinol* 2009; **1**:72–6.
5 Krieg T, Aumailley M. The extracellular matrix of the dermis: flexible structures with dynamic functions. *Exp Dermatol* 2011; **20**:689–95.
6 Yang CC, Cotsarelis G. Review of hair follicle dermal cells. *J Dermatol Sci* 2010; **57**:2–11.
7 Maryam Afshar M, Gallo RL. Innate immune defense system of the skin. *Vet Dermatol* 2013; **24**:32–9.
8 Kupper TS, Fuhlbrigge RC. Immune surveillance in the skin: mechanisms and clinical consequences. *Nat Rev Immunol* 2004; **4**:2011–22.

9 Streilein JS. Skin-associated lymphoid tissues (SALT): origins and functions. *J Invest Dermatol* 1983; **80**:12S–6S.

10 Bos JD, Zonneveld I, Das PK, Krieg SR, van der Loos CM, Kapsenberg ML. The skin immune system (SIS): its cellular constituents and their interactions. *Immunol Today* 1986; **7**:235–40.

11 Salmon JK, Armstrong CA, Ansel JC. The skin as an immune organ. *West J Med* 1994; **160**:146–52.

12 Nestle FO, Di Meglio P, Qin JZ, Nickoloff BJ. Skin immune sentinels in health and disease. *Nat Rev Immunol* 2009; **9**:679–91.

13 Luger TA, Schwarz T. Evidence for an epidermal cytokine network. *J Invest Dermatol* 1990; **95**(6 Suppl):100S–4S.

14 Sun protection. A Primary Teaching Resource. World Health Organization. 2003.

15 Matsumura Y, Ananthaswamy HN. Toxic effects of ultraviolet radiation on the skin. *Toxicol Appl Pharmacol* 2004; **195**:298–308.

16 Norval M, McLoone P, Lesiak A, Narbutt J. The effect of chronic ultraviolet radiation on the human immune system. *Photochem Photobiol* 2008; **84**:19–28.

17 Norval M. The mechanisms and consequences of ultraviolet-induced immunosuppression. *Prog Biophys Mol Biol* 2006; **92**:108–18.

18 Svobodova A, Walterova D, Vostalova J. Ultraviolet light induced alteration to the skin. *Biomed Pap Med Fac Univ Palacky Olomouc Czech Repub* 2006; **150**:25–38.

19 Scordi IA, Vincek V. Timecourse study of UVB-induced cytokine induction in whole mouse skin. *Photodermatol Photoimmunol Photomed* 2000; **16**:67–73.

20 Fisher MS, Kripke ML. Systemic alteration induced in mice by ultraviolet light irradiation and its relationship to ultraviolet carcinogenesis. *Proc Natl Acad Sci* 1977; **74**:1688–92.

21 Fisher MS, Kripke ML. further studies on the tumor-specific suppressor cells induced by ultraviolet radiation. *J Immunol* 1978; **121**:1139–44.

22 Ullrich SE, Kripke ML. Mechanisms in the suppression of tumor rejection produced in mice by repeated UV irradiation. *J Immunol* 1984; **133**:2786–90.

23 Gonzalez Maglio DH, Paz ML, Ferrari A, Weill FS, Czerniczyniec A, Leoni J, Bustamante J. Skin damage and mitochondrial dysfunction after acute ultraviolet B irradiation: relationship with nitric oxide production. *Photodermatol Photoimmunol Photomed* 2005; **21**:311–7.

24 Lee PL, van Weelden H, Bruijnzeel PL. Neutrophil infiltration in normal human skin after exposure to different ultraviolet radiation sources. *Photochem Photobiol* 2008; **84**:1528–34.

25 Köck A, Schwarz T, Kirnbauer R, Kirnbauer R, Urbanski A, Perry P, Ansel JC, Luger TA. Human keratinocytes are a source for tumor necrosis factor α: evidence for synthesis and release upon stimulation with endotoxin or ultraviolet light. *J Exp Med* 1990; **172**:1609–14.

26 Chung JH, Youn SH, Koh WS, Eun HC, Cho KH, Park KC, Youn JI. Ultraviolet B irradiation enhanced interleukin (IL)-6 production and mRNA expression are mediated by IL-1α in cultured human keratinocytes. *J Invest Dermatol* 1996; **106**:715–20.

27 Paz ML, Ferrari A, Weill FS, Leoni J, Maglio DH. Time-course evaluation and treatment of skin inflammatory immune response after ultraviolet B irradiation. *Cytokine* 2008; **44**:70–7.

28 González Maglio DH, Paz ML, Ferrari A, Weill FS, Nieto J, Leoni J. Alterations in skin immune response throughout chronic UVB irradiation—skin cancer development and prevention by naproxen. *Photochem Photobiol* 2010; **86**:146–52.

29 Ichihashi M, Ueda M, Budiyanto A, Bito T, Oka M, Fukunaga M, Tsuru K, Horikawa T. UV-induced skin damage. *Toxicology* 2003; **189**:21–39.

30 D'Orazio J, Jarrett S, Amaro-Ortiz A, Scott T. UV radiation and the skin. *Int J Mol Sci* 2013; **14**:12222–48.

31 Gläser R, Navid F, Schuller W, Jantschitsch C, Harder J, Schröder JM, Schwarz A, Schwarz T. UV-B radiation induces the expression of antimicrobial peptides in human keratinocytes *in vitro* and *in vivo*. *J Allergy Clin Immunol* 2009; **123**:1117–23.

32 Hong SP, Kim MJ, Jung MY *et al.* Biopositive effects of low-dose UVB on epidermis: coordinate upregulation of antimicrobial peptides and permeability barrier reinforcement. *J Invest Dermatol* 2008; **128**:2880–7.

33 Yano K, Kadoya K, Kajiya K, Hong YK, Detmar M. Ultraviolet B irradiation of human skin induces an angiogenic switch that is mediated by upregulation of vascular endothelial growth factor and by downregulation of thrombospondin-1. *Br J Dermatol* 2005; **152**:115–21.

34 Hirakawa S, Kodama S, Kunstfeld R, Kajiya K, Brown LF, Detmar M. VEGF-A induces tumor and sentinel lymph node lymphangiogenesis and promotes lymphatic metastasis. *J Exp Med* 2005; **201**:1089–99.

35 Kajiya K, Hirakawa S, Detmar M. Vascular endothelial growth factor-A mediates ultraviolet B-induced impairment of lymphatic vessel function. *Am J Pathol* 2006; **169**:1496–503.

36 McLoone P, Norval M. Adaptation to the UV-induced suppression of phagocytic activity in murine peritoneal macrophages following chronic exposure to solar simulated radiation. *Photochem Photobiol Sci* 2005; **4**:792–7.